$\mathrm{t}\bar{\mathrm{t}} + X$ hadroproduction at NLO accuracy with decay and evolution to the hadron level

Adam Kardos[1], *Maria Vittoria Garzelli*[2], *Zoltán Trócsányi*[1]

[1]Institute of Physics and MTA-DE Particle Physics Research Group, University of Debrecen, H-4010 Debrecen P.O.Box 105, Hungary
[2]Laboratory for Astroparticle Physics, University of Nova Gorica, SI-5000 Nova Gorica, Slovenia

DOI: `http://dx.doi.org/10.3204/DESY-PROC-2012-02/232`

We discuss how the hadroproduction of $\mathrm{t}\,\bar{\mathrm{t}}$-pairs in association with jets, vector and/or scalar bosons is implemented in the `PowHel` framework. In this framework matrix elements obtained from the `HELAC-NLO` package are used to provide predictions of distributions at the hadron level that are correct up to next-to-leading order accuracy in perturbation theory. We also show first predictions for $W^+W^-\mathrm{b}\,\bar{\mathrm{b}}$-hadroproduction.

Accurate predictions for the production of $\mathrm{t}\,\bar{\mathrm{t}}$-pairs alone or in association with jets, vector and/or scalar bosons are important for many experimental studies at hadron colliders both aiming at better understanding of the Standard Model (SM) and searches for new physics. However, the t-quarks and heavy bosons decay quickly and their decay products are detected. The experimental analyses often concentrate on the leptonic decay channels because these offer a much cleaner final state than the hadronic ones. Thus it is important not only to predict cross sections for the production of the heavy quarks and bosons, but also for the spectra of the leptons that emerge in their decays. While the theoretical description of such final states is straightforward at leading-order accuracy using the state-of-the art calculational tools, such predictions are known to suffer from large scale ambiguities and corrections from parton showers and hadronization. In order to improve the accuracy of the theoretical description during the last decade a lot of effort has been invested to match perturbative predictions at the next-to-leading order (NLO) accuracy with shower Monte Carlo (SMC) programs. One such approach is the POWHEG method [1, 2] that was implemented in a process independent framework in the `POWHEG-BOX` program [3].

To write the POWHEG cross section, one defines the NLO-corrected fully differential cross section belonging to the underlying Born configuration

$$\tilde{B}(\Phi_B) = B(\Phi_B) + V(\Phi_B) + \int \mathrm{d}\Phi_{\mathrm{rad}} \hat{R}(\Phi_R)\,,$$

and the POWHEG Sudakov form factor

$$\Delta(\Phi_B, p_\perp) = \exp\left\{ -\int \frac{\mathrm{d}\Phi_{\mathrm{rad}} R(\Phi_R)\Theta(k_\perp(\Phi_R) - p_\perp)}{B(\Phi_B)} \right\}\,.$$

In these equations $\mathrm{d}\Phi_B$ denotes the phase space measure of the Born computation, while $\mathrm{d}\Phi_R$ is that for the real radiation process. The latter is parametrized as $\mathrm{d}\Phi_R = \mathrm{d}\Phi_B \mathrm{d}\Phi_{\mathrm{rad}}$, where

$d\Phi_{\rm rad}$ includes the measure for the three variables that describe the radiation process of the extra parton and the corresponding Jacobian factor. The functions $B(\Phi_B)$ and $V(\Phi_B)$ denote the Born contribution and the finite part of the virtual corrections, respectively. Finally, $\hat{R}(\Phi_R)$ is the regularized real radiation contribution that is also defined in the FKS subtraction scheme. In the POWHEG-BOX the latter two are defined in the FKS subtraction scheme [4].

In the Sudakov form factor, the function $k_\perp(\Phi_R)$ has to be equal to the transverse momentum of the emitted parton relative to the emitting one near the region of singular emission. Then the POWHEG fully differential cross section is defined as

$$d\sigma_{\rm LHE} = \tilde{B}(\Phi_B) d\Phi_B \left[\Delta(\Phi_B, p_\perp^{\rm min}) + d\Phi_{\rm rad}\Delta\Big(\Phi_B, k_\perp(\Phi_R)\Big)\frac{R(\Phi_R)}{B(\Phi_B)}\Theta(k_\perp(\Phi_R) - p_\perp^{\rm min})\right] . \quad (1)$$

The advantage of this formula is that it can be used to generate equal weight events with Born configuration (first term) or including first radiation (second term). These events, termed LHE's, are stored in files according to the Les Houches accord [5].

The POWHEG-BOX provides a general framework to implement the POWHEG cross section in Eq. (1). In this framework, the following ingredients are needed:

- The flavor structures of the Born and real radiation emission subprocesses.
- The Born-level phase space, that we generate to emphasize the resonant kinematics of the decaying t- and $\bar{\rm t}$-quark.
- We obtain the squared matrix elements for the Born and the real-emission processes and color-correlated Born amplitudes with all incoming momenta using amplitudes computed by codes included in the HELAC-NLO package [6], in particular HELAC-1LOOP based on the OPP method [7] complemented by Feynman-rules for the computation of the QCD R_2 rational terms [8]. The matrix elements in the physical channels were obtained by crossing. In order to treat the numerical instabilities, we implemented dd-precision numerics by developing a HELAC-1LOOP@dd version of the HELAC-1LOOP program.
- We project spin-correlated Born amplitudes from the helicity basis to the Lorentz one by using the polarization vectors.

The generation of the matrix elements is straightforward using the HELAC-NLO code. There are two problems that arise during integration. The first one is that for vanishing transverse momentum of massless partons or vanishing invariant mass of a massless parton pair the Born cross section becomes singular. While this can never happen in a LO computation due to the selection cuts, it is a problem in the POWHEG method because the selection cuts can only be applied after event generation. The traditional way of treating this problem is the introduction of a generation cut. With this cut the LO cross section becomes finite, but the generation of the events is still rather inefficient because most of the events are generated in the region of small $p_\perp$ of the massless parton, thus they are lost when the physical selection cuts are applied (usually much higher, in the region of $20 - 30\,{\rm GeV}$). In order to make the generation of events more efficient, we introduce suppression factors. As we want to suppress the region of small $p_\perp$, our choice for the suppression factor is

$$\mathcal{F} = \left(\frac{p_\perp^2}{p_\perp^2 + p_{\perp,\,{\rm supp}}^2}\right)^i ,$$

with $i = 3$ in our calculation.

The second problem is a purely numerical one and is related to the numerical computation of one-loop amplitudes as implemented in `CutTools` [10]. In order to control numerical instabilities an $\mathcal{N}=\mathcal{N}$ test was implemented. For a given numerator we determine the scalar-integral coefficients using double precision arithmetics. We check the accuracy of the integrand by reconstructing it using all coefficients (and spurious terms) with a randomly chosen loop momentum. If the reached relative accuracy is worse than 10^{-4}, we pass the same phase space point in double-double precision (computed at the first place) to `HELAC-1LOOP@dd` to recalculate all the coefficients. The `HELAC-1LOOP@dd` code is a straightforward extension of `HELAC-1LOOP` to double-double precision using `QD` [9]. If the $\mathcal{N}=\mathcal{N}$ test fails, `CutTools` turns on its multi-precision version and calls the corresponding double-double precision version subroutines of `HELAC-1LOOP@dd`. This way we avoided all numerical instabilities in the computation of the virtual corrections.

We implemented all these improvements in the `PowHel` framework that can be used to generate LHE's for the following final states in hadroproduction: (i) a $\mathrm{t}\,\bar{\mathrm{t}}$-pair, (ii) a $\mathrm{t}\,\bar{\mathrm{t}}$-pair in association with a jet [11], (iii) a $\mathrm{t}\,\bar{\mathrm{t}}$-pair in association with a scalar [12] and a pseudoscalar Higgs boson [13], (iv) a $\mathrm{t}\,\bar{\mathrm{t}}$-pair in association with a SM Z^0-boson [14, 15], (v) $W^+W^-\mathrm{b}\,\bar{\mathrm{b}}$, and three more processes that are not yet published. In this proceedings we discuss item (v) briefly.

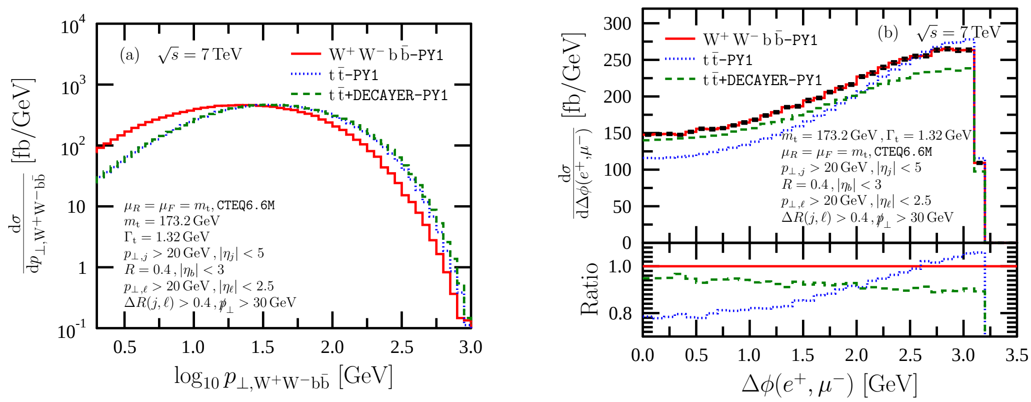

Figure 1: Distribution of the a) transverse momentum of the $W^+W^-\mathrm{b}\,\bar{\mathrm{b}}$-system; b) azimuthal separation between the hardest isolated positron and muon. The lower inset in the right panel shows the ratio of the predictions with approximate decays of the t-quarks as compared to the complete $W^+W^-\mathrm{b}\,\bar{\mathrm{b}}$-prediction. Selection cuts are specified in the plots.

Fig. 1.a shows the distribution of the transverse momentum of the $W^+W^-\mathrm{b}\,\bar{\mathrm{b}}$ system. Our selection cuts are shown in the figure. In a fixed-order computation this distribution diverges for vanishing transverse momentum. In the POWHEG cross section this divergence is smeared by the Sudakov form factor as can be seen in the figure. In addition to the $W^+W^-\mathrm{b}\,\bar{\mathrm{b}}$ final state computed at the NLO accuracy and matched to the `PYTHIA` SMC [16], we also show the prediction obtained by computing the $\mathrm{t}\,\bar{\mathrm{t}}$ final state and letting the SMC decay the heavy quarks (line marked as $\mathrm{t}\,\bar{\mathrm{t}}$-`PY1`). The third line (marked as $\mathrm{t}\,\bar{\mathrm{t}}$-`DECAYER-PY1`) shows the predictions obtained by performing the decays of the heavy particles according to the method descibed by Ref. [17] and implemented in a general way in our code `DECAYER`. The large difference between

the $W^+W^-\mathrm{b}\,\bar{\mathrm{b}}$-prediction is due to the different source of first emission in the two approaches: for the $W^+W^-\mathrm{b}\,\bar{\mathrm{b}}$-case first emission comes mainly from the b-quarks, that we treat as massless, while in the $\mathrm{t}\,\bar{\mathrm{t}}$-case first emission comes from the heavy t-quarks. As a result the latter spectra are much harder.

In Fig. 1.b we show the distribution of azimuthal separation between the hardest isolated positron and the muon. This distribution is an example where the differences between the three cases were clearly visible in the LHE's. These differences are only slightly altered by the PS, or the full SMC. In particular, the effect of including the spin-correlation leads to an increase of the distribution for small azimuthal separation $\Delta\phi_{e^+\mu^-}$, where the distribution from the $\mathrm{t}\,\bar{\mathrm{t}}$+`DECAYER` computation, which includes the spin correlations in an approximate way, and from the $W^+W^-\mathrm{b}\,\bar{\mathrm{b}}$-prediction are similar in shape. Only the normalizations of the two predictions differ due to the the singly- and non-resonant graphs that are absent in the $\mathrm{t}\,\bar{\mathrm{t}}$+`DECAYER` computation. For small separations, these are both significantly larger than the distribution $\mathrm{t}\,\bar{\mathrm{t}}$-`PY1` obtained from the $\mathrm{t}\,\bar{\mathrm{t}}$ events if the decay of the t-quarks is performed by the SMC, where spin correlations are neglected. At large separations however, the latter becomes even larger than the predictions from the $W^+W^-\mathrm{b}\,\bar{\mathrm{b}}$ computation.

This research was supported by the LHCPhenoNet network PITN-GA-2010-264564, the TÁMOP 4.2.1./B-09/1/KONV-2010-0007 and 4.2.2/B-10/1-2010-0024 projects, the Hungarian Scientific Research Fund grant K-101482. We are grateful to G. Bevilacqua, M. Worek, A. van Hameren and P. Skands for useful discussions.

References

[1] P. Nason. JHEP **0411** (2004) 040, arXiv:hep-ph/0409146 [hep-ph].

[2] S. Frixione, P. Nason, and C. Oleari. JHEP **11** (2007) 070, arXiv:0709.2092 [hep-ph].

[3] S. Alioli, P. Nason, C. Oleari, and E. Re. JHEP **06** (2010) 043, arXiv:1002.2581 [hep-ph].

[4] S. Frixione, Z. Kunszt, and A. Signer. Nucl.Phys. **B467** (1996) 399–442, arXiv:hep-ph/9512328 [hep-ph].

[5] E. Boos, M. Dobbs, W. Giele, I. Hinchliffe, J. Huston, *et al.* arXiv:hep-ph/0109068 [hep-ph].

[6] G. Bevilacqua, M. Czakon, M. V. Garzelli, A. van Hameren, A. Kardos, *et al.* arXiv:1110.1499 [hep-ph].

[7] G. Ossola, C. G. Papadopoulos, and R. Pittau. Nucl.Phys. **B763** (2007) 147–169, arXiv:hep-ph/0609007 [hep-ph].

[8] P. Draggiotis, M. V. Garzelli, C. G. Papadopoulos, and R. Pittau. JHEP **0904** (2009) 072, arXiv:0903.0356 [hep-ph].

[9] Y. Hida, X. S. Li, and D. H. Bailey, "Quad-double arithmetic: Algorithms, implementation, and application", Tech. Rep. LBNL-46996, Lawrence Berkeley National Laboratory, Berkeley, CA 94720, October, 2000. Available at http://www.nersc.gov/~dhbailey/mpdist/mpdist.html.

[10] G. Ossola, C. G. Papadopoulos, and R. Pittau. JHEP **03** (2008) 042, arXiv:0711.3596 [hep-ph].

[11] A. Kardos, C. G. Papadopoulos, and Z. Trocsanyi. Phys.Lett. **B705** (2011) 76–81, arXiv:1101.2672 [hep-ph].

[12] M. V. Garzelli, A. Kardos, C. G. Papadopoulos, and Z. Trocsanyi. Europhys.Lett. **96** (2011) 11001, arXiv:1108.0387 [hep-ph].

[13] S. Dittmaier, C. Mariotti, G. Passarino, R. Tanaka, *et al.* arXiv:1201.3084 [hep-ph].

[14] A. Kardos, Z. Trocsanyi, and C. G. Papadopoulos. Phys.Rev. **D85** (2012) 054015, arXiv:1111.0610 [hep-ph].

[15] M. V. Garzelli, A. Kardos, C. G. Papadopoulos, and Z. Trocsanyi. Phys.Rev. **D85** (2012) 074022, arXiv:1111.1444 [hep-ph].

[16] T. Sjostrand, S. Mrenna, and P. Z. Skands. JHEP **0605** (2006) 026, arXiv:hep-ph/0603175 [hep-ph].

[17] S. Frixione, E. Laenen, P. Motylinski, and B. R. Webber. JHEP **04** (2007) 081, arXiv:hep-ph/0702198.